Title
Elastomeric composites for flexible microwave substrates

Journal
Journal of Applied Physics, 119(12)

ISSN
0021-8979

Authors
Awang, Robiatun A
Baum, Thomas
Berean, Kyle J
et al.

Publication Date
2016-03-28

DOI
10.1063/1.4945037

JOURNAL OF APPLIED PHYSICS **119**, 124109 (2016)

Elastomeric composites for flexible microwave substrates

Robiatun A. Awang,[1,2,a)] Thomas Baum,[1] Kyle J. Berean,[1] Pyshar Yi,[1] Kourosh Kalantar-zadeh,[1] Sharath Sriram,[1,2] and Wayne S. T. Rowe[1,a)]
[1]*School of Engineering, RMIT University, Melbourne, Victoria 3001, Australia*
[2]*Functional Materials and Microsystems Research Group and Micro Nano Research Facility, RMIT University, Melbourne, Victoria 3001, Australia*

(Received 21 December 2015; accepted 18 March 2016; published online 31 March 2016)

Manipulating dielectric properties of polydimethylsiloxane (PDMS) is an important consideration for flexible, low-loss device design. This paper presents a method for reducing dielectric loss (tan δ) by forming PDMS composites loaded with various concentrations of either alumina (Al_2O_3) or polytetrafluoroethylene (PTFE) particles. The structural, mechanical, and electrical properties of the composites are investigated. Theoretical mixing models were used to predict the relative permittivity (ε_r) of PDMS composites, and good similarity with the measured ε_r was observed. The incorporation of either low dielectric loss filler in the PDMS matrix (up to 50 wt. % filler loading) is shown to reduce the dielectric loss while maintaining the flexibility of the host matrix. The fillers can also control the permittivity of the composite, either increasing or decreasing relative permittivity from that of PDMS. Interestingly, a strain of ~500% can be applied to 15 wt. % PDMS/PTFE composites, compared with ~350% for pure PDMS. © *2016 AIP Publishing LLC*.
[http://dx.doi.org/10.1063/1.4945037]

I. INTRODUCTION

The demand for flexible, low-loss substrates for microwave frequencies is increasing, with many examples presented for radio-frequency (RF) switching/tuning mechanisms[1,2] and biomedical applications.[3] However, it is very difficult to identify a homogeneous material which possesses these desired properties. Alternatively, polymer-ceramic composites are commonly proposed, as most polymers like silicone rubber, butyl rubber, and fluoro-polymer offer excellent flexibility at low cost, while several ceramics have low dielectric loss properties.[4–8]

The challenges associated with creating polymer-ceramic composites to form flexible-low loss materials often stem from inhomogeneous distribution of the fillers within the polymer host-matrix, and compatibility between the fillers and the polymer. Among the existing polymers, polydimethylsiloxane (PDMS) has been extensively used to fabricate stretchable microwave devices like resonators, antennas, switches, filters, and oscillators.[9–11] PDMS polymer nanocomposites have also been employed for many other diverse functions and applications.[12–15] In general, the dielectric properties of the composite depend on structure, size, morphology, and concentration of filler loadings.[16,17] However, PDMS exhibits significant dielectric loss at microwave frequencies, which limits its application for use as a flexible dielectric material.

Numerous polymer-ceramic composites have been reported to demonstrate flexible substrates.[5,10,17–22] Koulouridis *et al.* presented flexible substrates for antenna and filter design at microwave frequencies made from composites of PDMS and various ceramic powders, namely, barium titanate (BT: $BaTiO_3$), Mg-Ca-Ti (MCT), and Bi-Ba-Nd-titanate (BBNT).[10] At 1 GHz, the loss tangent of the BT/PDMS composite was comparatively higher (tan δ of 0.04) than the loss tangent of MCT/PDMS and BBNT/PDMS composites (tan $\delta < 0.009$) for 0.25 volume fraction of the ceramic. A microwave antenna and filter were constructed using the developed composites. However, the structural performance of these composites has not been quantified.

Namitha *et al.* recently studied the effect of particles size on the microwave properties of silicone rubber-alumina composites.[17] Nano-size Al_2O_3 (alumina) fillers were shown to produce increasingly higher dielectric loss with respect to the filler loading, which contradicts perceived trends about such mixtures. The increment of dielectric loss was reported to be due to higher moisture contents and the large interface area of the nano-alumina particles. In addition, the nano-size alumina-filled silicone rubber composite produced better mechanical properties than micro-sized alumina fillers. However, the investigation is limited to a relatively low volume fraction (0.05%) of nano-alumina filler due to issues with the mixing process for higher filler loadings. Alumina-filled Butyl Rubber composites are studied by Chameswary *et al.*;[4] however, the study also uses a low volume fraction of 0.1 for the nano-alumina filler.

Polytetrafluoroethylene (PTFE) has been extensively used as matrix polymer and mixed with several ceramic fillers to form microwave dielectric composites.[5,20,21] A comparison of alumina- and magnesia-filled PTFE composites in terms of dielectric, structural, microstructure, and moisture absorption properties was reported by Murali *et al.*[21] Alumina and magnesia were chosen because of their almost identical dielectric properties. The loss tangent of both composites also showed an increasing trend with respect to filler loading up 60 wt. %, with PTFE/magnesia composites exhibiting high loss tangent values compared with the corresponding PTFE/alumina composite. No measurements have been

[a)]Electronic addresses: s3391611@student.rmit.edu.au and wayne.rowe@rmit.edu.au.

conducted to study the mechanical properties and flexibility of the proposed composites. Recently, PDMS-PTFE membrane composite was fabricated for pervaporation of chloroform[23] and the structural, mechanical, and thermal properties were studied. Nevertheless to-date, a gap exists in the literature in identifying the dielectric properties of composites using PTFE as filler for flexible electronics applications at microwave frequencies.

This paper studies the effects of two low dielectric loss fillers within a PDMS matrix on the structural, mechanical, and dielectric properties of the resulting composite. Alumina (ε_r: ~10, $\tan\delta$: ~0.0003 at 10 GHz) and PTFE (ε_r: ~2.1, $\tan\delta$: ~0.0004 at 10 GHz) are chosen fillers since both of them have lower dielectric loss than the PDMS matrix. Alumina has higher ε_r, while PTFE has a lower ε_r than the PDMS; hence, controlled mixtures can also be used to tailor the relative permittivity of the composite. Experimentally obtained values of ε_r are compared with the Maxwell-Garnet, Lichtenecker, and Effective Medium theoretical (EMT) mixing laws. Furthermore, the structural and mechanical properties of PDMS/alumina and PDMS/PTFE composites are examined up to 50 wt. % filler loading.

II. EXPERIMENTAL SECTION

A. Material and composite sample preparations

To investigate the impact of the composite fillers on the permittivity and dielectric loss of PDMS, the following preparation process was used. Dow Corning's Sylgard 184™ PDMS with relative permittivity (ε_r) of 2.68 and dielectric loss ($\tan\delta$) of 0.00133 at 100 kHz was selected as the host phase because it has been commonly used in practical applications.[1,9,11] The properties of PDMS have been measured using a coaxial dielectric probe (Agilent Technologies, Model 85070E) to give $\varepsilon_r = 3.0$ and $\tan\delta = 0.05$ at 3.45 GHz.[24] At frequencies up to 20 GHz, PDMS has the reported properties of $\varepsilon_r = 2.72$ and loss ranging from 0.0366 to 0.0433 (0.055–0.065 dB cm^{-1} GHz^{-1}).[11] The properties can be dependent on the preparation process. Hence, in this work, the composites will be benchmarked against measured values of PDMS prepared in the same fashion. Alumina nanoparticles (average dimension <50 nm) and PTFE microparticles (average dimension <10 μm) purchased from Sigma-Aldrich, Australia were used as the filler phase. The alumina nanoparticles were pre-baked at 100 °C for seven days to remove any additional moisture content which could introduce additional loss in the resulting composite.

The mixing process begins with the preparation of PDMS by adding one part (by weight) of a proprietary curing/cross-linking agent (Sylgard 184, Dow Corning Corporation) to ten parts (by weight) of PDMS pre-polymer. The desired amount of filler particles was added to the PDMS mixture and heavy stirring by hand was applied for 10 min. Because of higher filler loadings (particularly the 50 wt. %), a magnetic stirrer or any other controllable stirrer cannot be used as the mixture forms a thick paste. The obtained PDMS composites were degassed in a vacuum oven for ~1 h to remove air bubbles. The resulting fully degassed mixture was molded into bar-shape of 3.2 mm × 3.2 mm × 10 mm size and cured for solidification at room temperature for ~24 h. The sample dimensions were prepared to suit the dielectric measurement procedure using the waveguide resonant cavity method. Samples with filler concentration of 15 wt. % (4.35 vol. %), 30 wt. % (9.94 vol. %), and 50 wt. % (20.48 vol. %) for PDMS/alumina composites and 15 wt. % (7.80 vol. %), 30 wt. % (17.03 vol. %), and 50 wt. % (32.39 vol. %) for PDMS/PTFE composites were prepared using this method.

The same preparation steps were applied to create samples for tensile strain, moisture absorption, density, and swelling measurements. For the tensile stress-strain measurement, a composite sheet of ~2 mm thickness was prepared. The composite sheets were die cut into dumb-bell shapes with an overall length of 75 mm, a 30 mm long narrow section with a width of 4 mm, and a gauge width of 12 mm. For the moisture absorption, density, and swelling measurements, a sample dimension of 3.2 mm × 3.2 mm × 20 mm size was used.

B. Characterization

The microstructure of the composites was examined using an environmental scanning electron microscope (ESEM, FEI Quanta 200). The tensile stress-strain of pure PDMS, PDMS/alumina nanocomposites, and PDMS/PTFE microcomposites were measured using a Universal Testing Machine (UTM; WL 2100; Instron, Norwood, MA) with a rate of grip separation of 500 mm/min.

Archimedes' principle was used to determine the density of the composites.[25] The samples were dried for 1 h at 110 °C in an oven and weighed in air (W_{air}). Then, they were carefully immersed in 2-propanol fluid and immediate weight was taken ($W_{2\text{-propanol}}$). The measured density of the composite was calculated using the following equation:

$$\rho_{mea} = \frac{W_{air}\rho_{2-propanol}}{W_{air} - W_{2-propanol}}, \tag{1}$$

where ρ_{mea} is the measured density of the composite, $\rho_{2-propanol}$ is the density of 2-propanol fluid of 0.789 g/cm^3, W_{air} is the weight of the sample in air, and $W_{2\text{-}propanol}$ is the weight of the sample in 2-propanol fluid.

The dielectric properties of the PDMS composites were measured using a rectangular waveguide cavity resonant method. The cavity was custom-built to resonate at approximately 10 GHz using a section of WR-90 waveguide with irises at either end, as shown in Figure 1. Although the results are at single frequency, they should not vary greatly over X-band (8–12 GHz). A bar-shaped sample is located in the position of the maximum electric field for the TE_{107} mode, causing a shift of the resonant frequency and a decrease of the quality factor of the cavity. The real (ε'_r) and imaginary (ε''_r) parts of the PDMS composite permittivity can then be calculated from the changes of the resonant frequency and quality factor of the cavity, respectively.[26] The dielectric loss ($\tan\delta$) is the ratio of imaginary part to the real part of the permittivity

$$\varepsilon'_r = \frac{V_c(f_c - f_s)}{2V_s f_s} + 1, \tag{2}$$

$$\varepsilon''_r = \frac{V_c}{4V_s}\left(\frac{1}{Q_s} - \frac{1}{Q_c}\right), \tag{3}$$

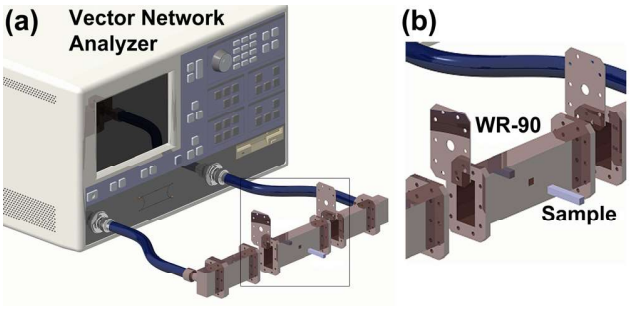

FIG. 1. Experimental setup for dielectric property measurement of PDMS composites. (a) The interfacing of the WR-90 waveguide to the vector network analyzer is shown. (b) A magnified view of the boxed region in (a) showing the position of the sample in the waveguide.

where f_c and f_s are the resonant frequencies, Q_c and Q_s are the quality factors of the cavity without and with the sample inside the cavity, respectively, and V_c and V_s are the volumes of the cavity and sample, respectively. The validity of the experimental setup is determined by measuring a standard made of Rogers RT/Duroid 5880 material. To ensure the repeatability and accuracy of the measurement, five different samples of each individual composite are measured, and the average value of dielectric permittivity and loss tangent was calculated and plotted.

For calculating the ε_r using the theoretical mixing laws,[20,27] the volume fraction (V_f) of alumina and PTFE particles for a given weight fraction (W_f) can be determined using the equation

$$V_f = \frac{W_f}{W_f + W_m(\rho_f/\rho_m)}, \tag{4}$$

where ρ_f is the density of the filler particles, and W_m and ρ_m are the weight fraction and density of PDMS matrix, respectively.

Moisture absorption of the composites was also measured. Test samples were initially desiccated at 110 °C for 1 h in an oven. Weight of the samples was taken in air and then submerged in deionized water at room temperature 25 °C for 24 h. The specimens were taken out and the excess water from the surface was removed by carefully wiping with a dry cloth followed by immediate weighing. The water absorption of the composite is calculated from the weight gain.

Solvent swelling measurements were also carried out. Test samples were initially pre-weighed and then totally immersed in pure toluene at room temperature (25 °C) for 24 h until equilibrium swelling was reached. The swollen samples were then taken out and, after the excess toluene from the surface was carefully removed by wiping with a dry cloth, immediately weighed. To ensure repeatable results, the measurement was repeated three times.

III. RESULTS AND DISCUSSION

A. SEM of the PDMS composites

Figure 2 presents scanning electron micrographs of PDMS/alumina composites for 15, 30, and 50 wt. %, respectively. Further images for multiple samples of each composite are included in the supplementary material[28] (see Figure S1 of supplementary material). It can be seen that alumina particles are uniformly dispersed throughout the PDMS matrix, validating the effectiveness of the manual stirring method. As the filler content increases, the agglomeration also increases, as evident in Figure 2(c).

In Figure 3, micrographs of PDMS/PTFE composites with different weight fractions of the micro-PTFE filler are shown, with additional images supplied in the supplementary material[28] (see Figure S2 of supplementary material). Figure 3(a) indicates that PTFE particles have an average size of $<10\,\mu$m. As the filler content increases, particle agglomeration appears and air inclusions also arise.

B. Density

Figure 4 demonstrates the variation in the calculated and measured values of the density for PDMS/alumina and PDMS/PTFE composites verses weight fraction. The uncertainties for

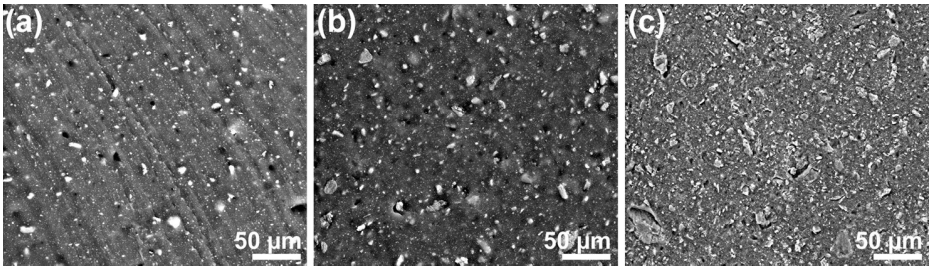

FIG. 2. Cross-sectional electron micrographs of PDMS/alumina composites with filler concentrations of: (a) 15 wt. %, (b) 30 wt. %, and (c) 50 wt. %.

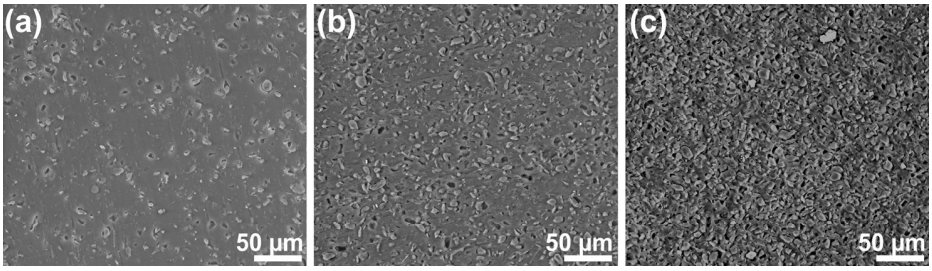

FIG. 3. Cross-sectional electron micrographs of PDMS/PTFE composites with filler concentrations of: (a) 15 wt. %, (b) 30 wt. %, and (c) 50 wt. %.

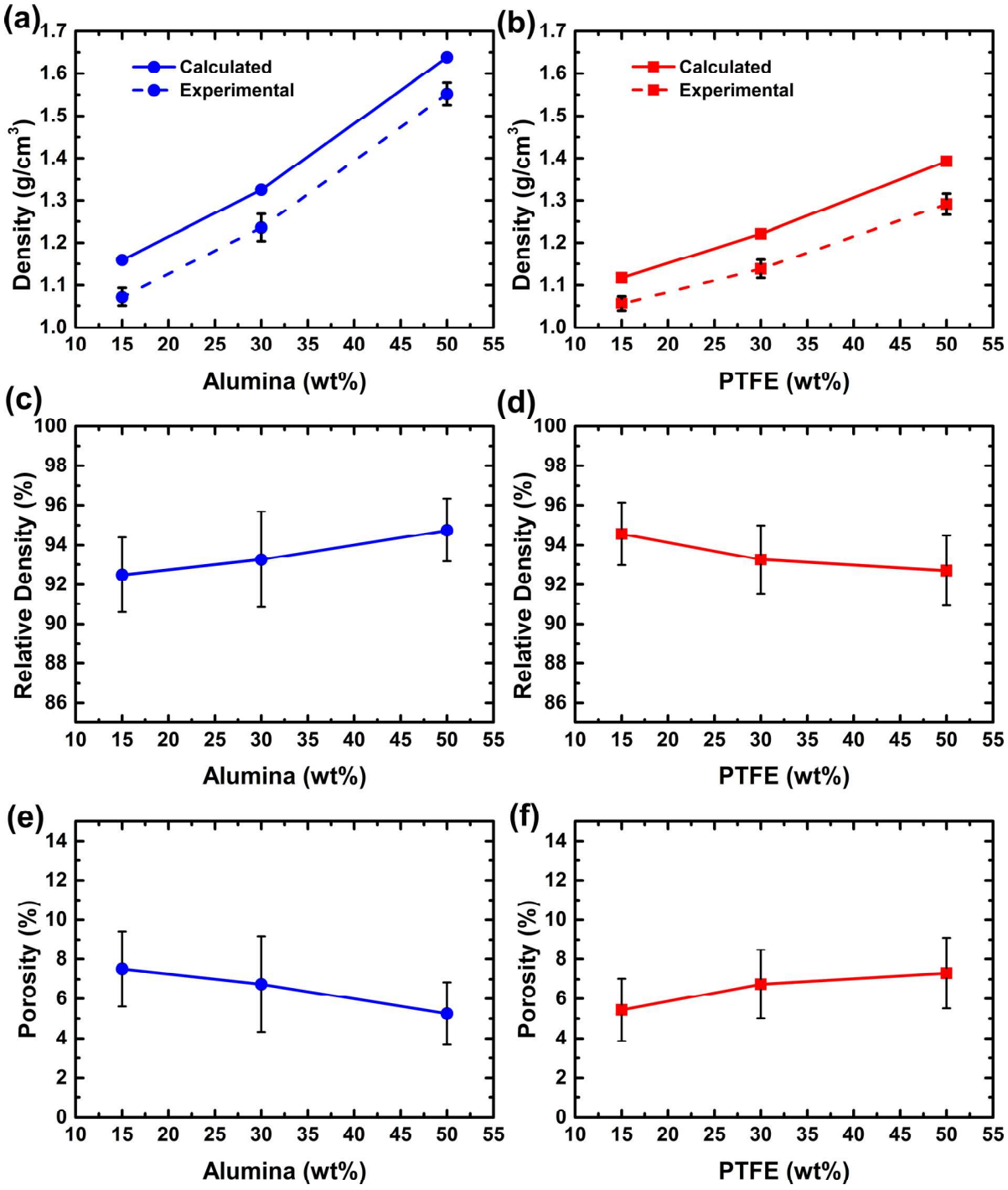

FIG. 4. (a) and (b) Measured and calculated density of composites at different weight fractions of filler. (c) and (d) Calculated relative density of PDMS/alumina composites and PDMS/PTFE composites, respectively. (e) and (f) Calculated porosity of PDMS/alumina composites and PDMS/PTFE composites.

the measured density for both composites are around ±2.5%. The calculated values of the density of composites, ρ_{cal}, are obtained using equation[29]

$$\rho_{cal} = \rho_f V_f + \rho_m (1 - V_f), \tag{5}$$

where ρ_{f} and ρ_{m} are the density of the filler and the matrix, respectively, and V_f is the volume fraction of the filler.

The values of ρ_{cal} and average measured density (ρ_{mea}) exhibit a similar increasing trend with greater filler loadings, since the density of both alumina ($\rho_f = 4\,\mathrm{g/cm^3}$) and PTFE ($\rho_f = 2.15\,\mathrm{g/cm^3}$) is higher than that of cured PDMS ($\rho_m = 1.03\,\mathrm{g/cm^3}$). However, the ρ_{mea} is smaller than the calculated density at specific weight fractions of the fillers. This is a result of the formation of pores in the composites which is not considered in the calculated values. The porosity, p, of composites can be calculated from the measured and calculated density of composites[20]

$$p = 1 - \frac{\rho_{mea}}{\rho_{cal}} = 1 - \rho_{rel}, \tag{6}$$

where ρ_{rel} is the relative density of the composites. The porosity of PDMS/alumina composites decreases as filler loading increases indicating the good compatibility and uniform blending between the PDMS matrix and alumina filler as in Figure 4(e). However, a contradictory trend is observed for PDMS/PTFE composites which implies the increasing void formation/air inclusion as the PTFE filler loading increases. This supports the observations of porosity in Figure 4(f). A ~7.3% porosity can be seen for 50 wt. % of PTFE filler loading.

C. Dielectric properties of the composites at microwave frequencies

The variation in relative permittivity and loss tangent of the composites as a function of alumina and PTFE filler loading in the PDMS matrix is shown in Figure 5. As ε_r of the alumina filler is higher than the PDMS matrix, the ε_r of PDMS/alumina composites shows an increasing trend with filler loading. A contrasting trend can be seen for the PDMS/PTFE composites due to slightly lower relative permittivity of PTFE compared with the PDMS matrix.

The dielectric loss of PDMS/alumina and PDMS/PTFE composites decreases as the filler weight fraction increases is shown in Figure 5. The lowest dielectric loss is achieved for 50 wt. % PDMS/alumina and 50 wt. % PDMS/PTFE composites, showing loss tangents of 0.018 and 0.017, respectively. We hypothesize that this is due to the lower dielectric loss of filler compared with the PDMS matrix at microwave frequencies. The decreasing trend of dielectric loss with the increment fillers loading up to 50 wt. % opposes the previous findings for the silicone-rubber/nano-alumina composites as reported by Namitha *et al.*[17] To further investigate and clarify this, two additional experiments were carried out. First, preparation of the PDMS-alumina composites without any pre-bake process and second, the nano-alumina particles were purposely left in a humid environment for 5 h to force the particles to absorb as much water as possible. The composites were then prepared and the dielectric properties were measured using the same method as described in Section II. In both cases, the measured of dielectric loss exhibits similar reduction trends with the incremental filler loading as the prolonged pre-bake findings, as can be seen in Figure 5(a). Even in the extreme case of deliberately humidifying the filler particles, we have been unable to reproduce the increase in loss reported by Namitha *et al.*, which they attributed to water absorption of the filler. This enhancement indicates that the incorporated PDMS composites are suitable to be implemented as microwave substrate for applications with the requirement for low dielectric loss.

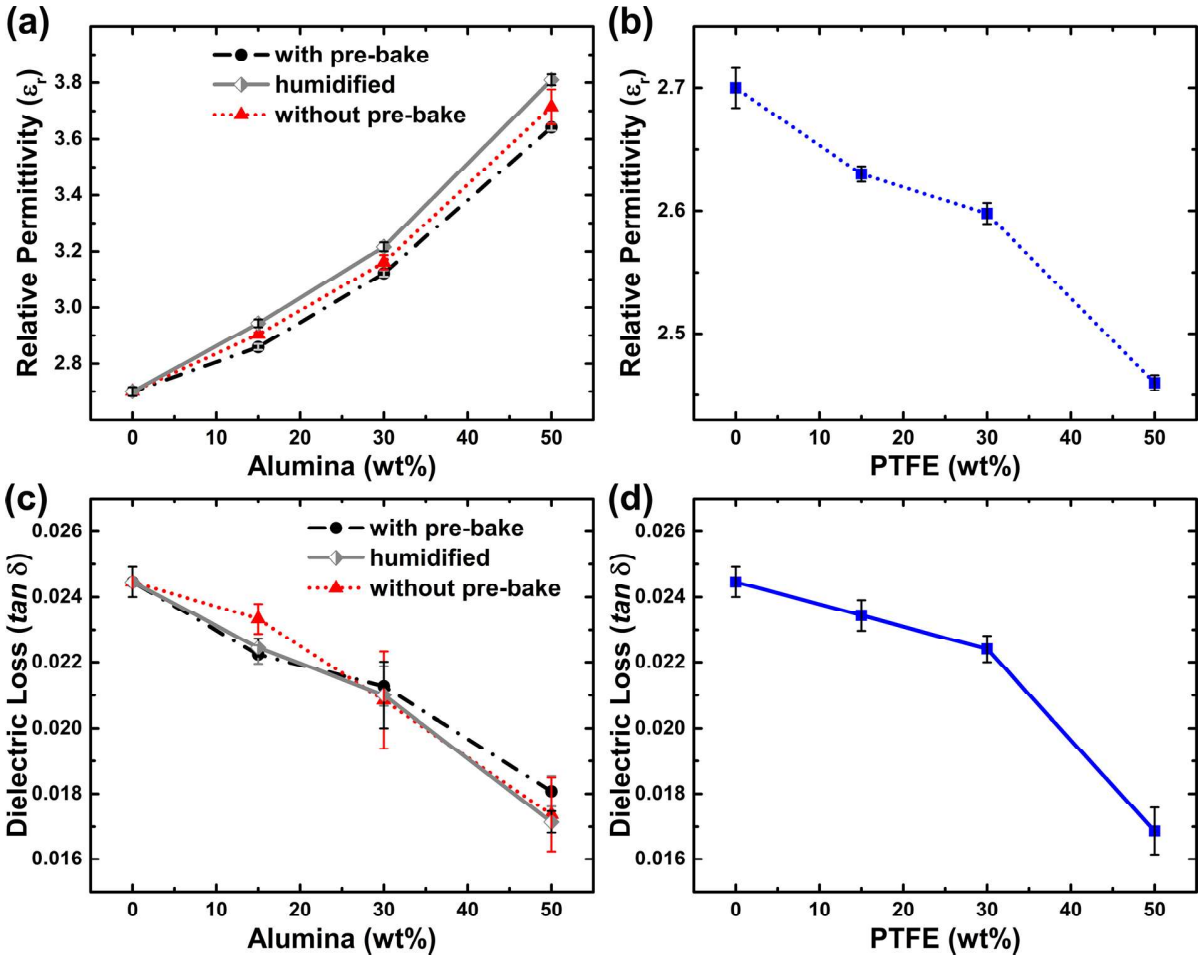

FIG. 5. (a) and (b) Variation of relative permittivity of composites with respect to the filler loading at 10 GHz. (c) and (d) Variation of loss tangent of composites with respect to the filler loading at 10 GHz.

The uncertainty of the resulting relative permittivity and loss tangent using the waveguide resonant cavity approach is calculated at ±2% and ±0.06%, respectively. These values are congruent with other reported results for this method.[30,31] Figure 5 also highlights the highest standard deviation of relative permittivity and loss tangent for PDMS/alumina composites without the pre-bake process. Hence, the uncertainty of the water content in the non-prebaked alumina filler has an impact on the characterization accuracy of the dielectric properties.

The following dielectric mixing law models are used to calculate the effective relative permittivity of PDMS-composites at 10 GHz.

Maxwell-Garnett model[20]

$$\frac{\varepsilon_{eff}-\varepsilon_m}{\varepsilon_{eff}+\varepsilon_m}=V_f\frac{\varepsilon_f-\varepsilon_m}{\varepsilon_f+\varepsilon_m}. \tag{7}$$

Lichtenecker model[27]

$$\ln\varepsilon_{eff}=V_f\ln\varepsilon_f+(1-V_f)\ln\varepsilon_m. \tag{8}$$

EMT model[32]

$$\varepsilon_{eff}=\varepsilon_m\left[1+\frac{V_f(\varepsilon_f-\varepsilon_m)}{\varepsilon_m+n(1-V_f)(\varepsilon_f-\varepsilon_m)}\right], \tag{9}$$

where ε_{eff}, ε_f, and ε_m are relative permittivity of composite, filler, and matrix, respectively, V_f is the volume fraction of the filler, and n is the morphology/shape factor. For the EMT model, the n is determined by empirical calculation where lower values signify filler particles of a near-spherical shape.

The predicted values of relative permittivity for PDMS/alumina and PDMS/PTFE composites are compared with the experimental results in Figure 6. For PDMS/alumina composites, the EMT model was found to have good agreement with the experimental results at n of 0.275. However, Maxwell-Garnett and Lichtenecker theoretical models match closely with experimental values at lower weight fractions of filler. Beyond 15 wt. %, the experimental relative permittivity slightly deviates from the theoretically predicted models. This can be attributed to the agglomeration of alumina particles at higher filler loading.[17]

For PDMS/PTFE composites, the experimental values present a small deviation from the predictions by all the theoretical models. This again may be due to the increase in agglomeration as a result of higher filler loading in the PDMS matrix. However, the relative deviation between predicted and experimental values for both composites is <2%. Both composites exhibit small deviations at higher filler loading, due to agglomeration/air inclusions;[32,33] therefore, all the theoretical models used should only be considered as a rough estimator of relative permittivity for higher loadings.

D. Stress-strain measurement results

The characteristics stress-strain data of Figure 7 show that the tensile stress drops significantly with addition of fillers to the PDMS matrix. Increasing the alumina concentrations also decreases the elasticity/flexibility of PDMS/alumina composites

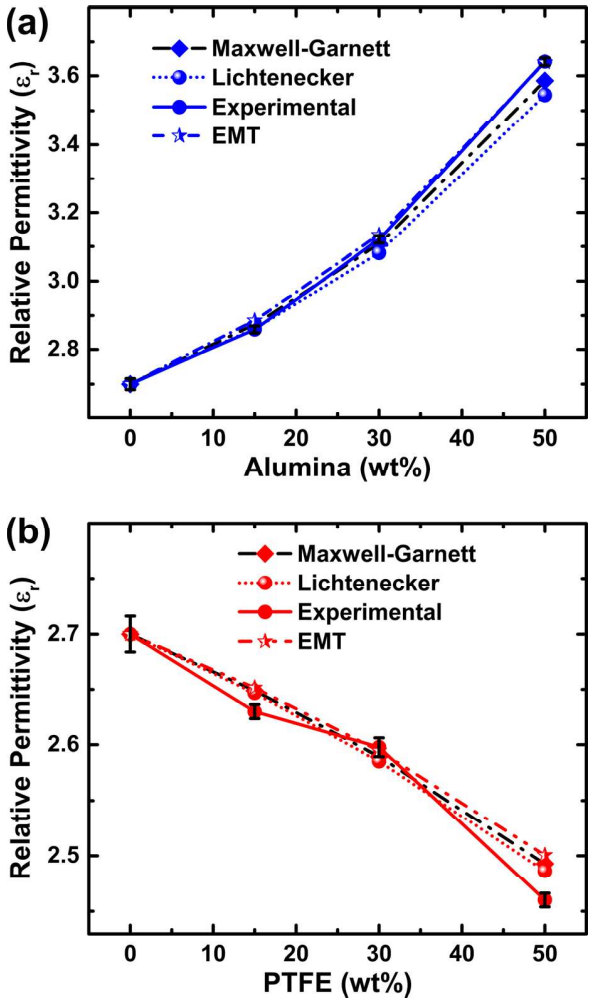

FIG. 6. Comparison of experimental and theoretical relative permittivity with respect to the filler loading. (a) PDMS/alumina composites and (b) PDMS/PTFE composites.

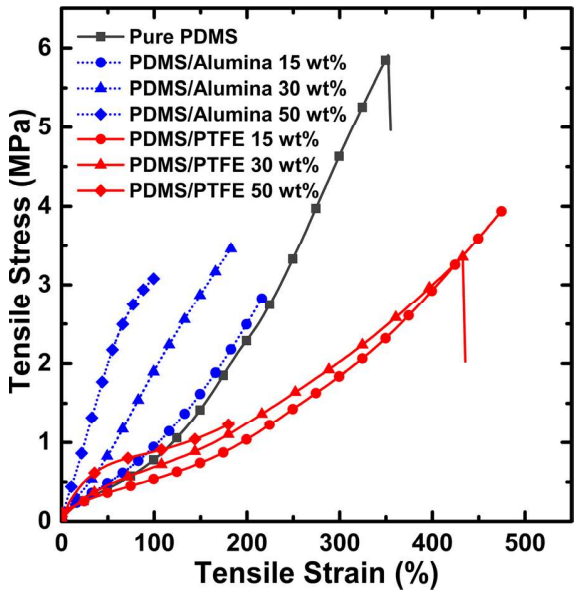

FIG. 7. Stress-strain relationship of PDMS composites.

as the presence of the alumina particles weakens the filler-matrix mixture interface. In the worst case, approximately 100% strain can be applied to 50 wt. % of PDMS/alumina composite before it breaks.

In contrast, the PDMS/PTFE composites exhibit an increasing flexibility for 15 wt. % and 30 wt. % of PTFE concentration as depicted in Figure 7. A strain of ~500% can be applied for 15 wt. % concentration, exceeding the 350% for pure PDMS. However, as the filler contents increases, the agglomerations also increase which may be the reason why less flexibility occurs at the higher filler loading (50 wt. %).

E. Moisture absorption

Moisture absorption is a major concern in microwave circuit applications since water will degrade the dielectric properties of composites substrate material and may cause damage to metallic tracks and other circuitry. Figure 8 indicates that as the filler loading increases, moisture absorption also increases. The highest deviation of moisture absorption is measured at higher filler loadings, with only ±0.1% variation. At 50 wt. % filler loading, PDMS/alumina composite and PDMS/PTFE composite have a moisture absorption of 0.20% and 0.45%, respectively. For the PDMS/alumina composites, the slightly increased moisture absorption is due to agglomeration and hydrophilic nature of ceramic fillers. However, for the PDMS/PTFE composites which exhibit superhydrophobic behavior,[34] the increasing trend of moisture absorption with respect to filler loading concentrations is likely due to increase of porosity/air inclusions in the microstructure which has been identified by examining the composite density in Figure 4(f).

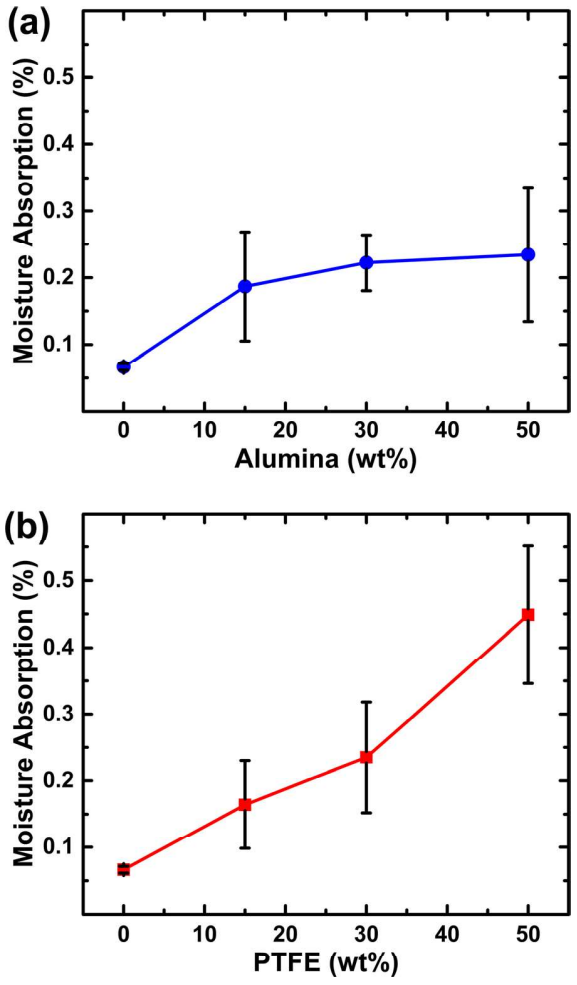

FIG. 8. Moisture absorption of the composites with respect to the filler loading. (a) PDMS/alumina composites and (b) PDMS/PTFE composites.

F. Swelling measurements

Equilibrium swelling measurements of the composite were investigated and compared with a pristine PDMS reference to evaluate any changes in cross-linking density.[35] The solvent uptake, or mass swelling degree (MSD), is presented in Figure 9. The MSD of pristine PDMS published in the previous studies is in agreement with the obtained result.[36,37]

Figure 9 shows the MSD decreases with the increase of alumina or PTFE filler loadings. It also reveals a steep decrease in the MSD for PDMS/alumina composites compared with PDMS/PTFE composites at the same weight fraction loading. At a filler loading of 50 wt. %, a decrease in MSD of approximately 65% and 22% is observed for PDMS/alumina and PDMS/PTFE composites, respectively. The reduction of MSD implies an increasing cross linking density which is associated with a decreasing chain length between the cross-links within the polymer.[38]

The MSD of PDMS/alumina composites in Figure 9 shows a large difference/reduction with respect to what the theoretical calculation of MSD would be if the crosslinking density of the PDMS remained constant. The substantial reduction of MSD was associated with higher cross linking density, producing shorter chain length and therefore a tighter polymeric matrix. This also causes a reduction in the elasticity/flexibility of PDMS/alumina composites, as confirmed through the stress-strain measurements seen in Figure 7.

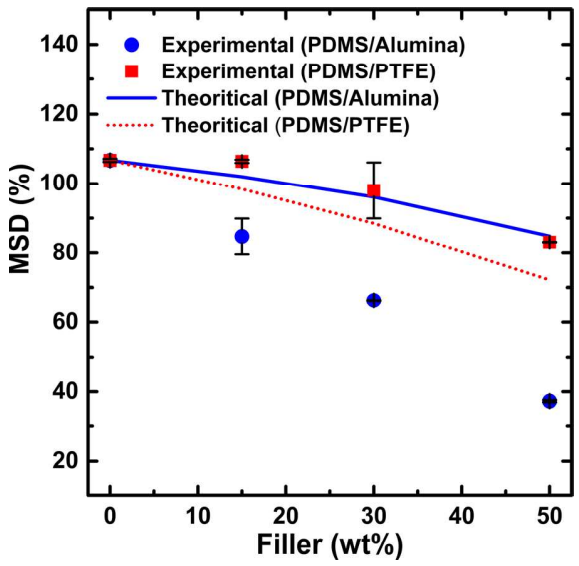

FIG. 9. Cross-linking study of the PDMS/alumina and PDMS/PTFE composites at different weight fractions of filler based on mass swelling degree (MSD).

The PDMS/PTFE composites show a contrasting result for MSD implying a reduction in crosslinking density of the base PDMS. The measured MSD is slightly higher than the theoretical MSD which can be ascribed to a reduction in crosslinking density, creating a looser polymeric matrix. Consequently, the PDMS/PTFE composites (15 wt. % and 30 wt. %) are more flexible than pure PDMS as verified by the tensile strain of Figure 7. However, the lower flexibility the 50 wt. % of PDMS/PTFE composite can be attributed to particle agglomeration as confirmed in SEM image of Figure 3(c).

IV. CONCLUSION

The properties of PDMS/alumina and PDMS/PTFE composites have been examined in terms of their structural, dielectric, and mechanical properties. Scanning electron micrographs reveal an occurrence of agglomeration and air inclusions with increasing of filler loadings for both composites, in particular, the PDMS/PTFE composites. The density was measured and the porosity calculated as confirmation. The experimental relative permittivity of both composites exhibits control over the dielectric properties and is in good agreement with the predicted theoretical models. Increases/decreases in relative permittivity corresponded to the addition of more alumina/PTFE into the PDMS as hypothesized. Dielectric loss tangent was also shown to decrease with filler loading. At 50 wt. % filler loading, the loss tangent was 0.018 and 0.017 for PDMS/alumina and PDMS/PTFE composites, respectively. The PDMS/PTFE composites exhibited higher flexibility/elasticity compared with PDMS/alumina composite as supported by mass swelling degree results. However, both composites had an increasing trend of moisture absorption with respect to the filler loading. The study shows that PDMS/alumina and PDMS/PTFE composites offer a potential solution for flexible microwave substrate applications.

ACKNOWLEDGMENTS

The authors acknowledge the facilities and technical assistance of the Australian Microscopy & Microanalysis Research Facility at RMIT University. The authors also would like to acknowledge Ministry of Education (MOE), Malaysia and Universiti Teknologi MARA, Malaysia for the financial assistance.

[1]J.-H. So, J. Thelen, A. Qusba, G. J. Hayes, G. Lazzi, and M. D. Dickey, Adv. Funct. Mater. **19**, 3632 (2009).
[2]Z. Sheng and V. V. Varadan, J. Appl. Phys. **101**, 014909 (2007).
[3]M. L. Scarpello, D. Kurup, H. Rogier, D. Vande Ginste, F. Axisa, J. Vanfleteren, W. Joseph, L. Martens, and G. Vermeeren, IEEE Trans. Antennas Propag. **59**, 3556 (2011).
[4]J. Chameswary, L. K. Namitha, M. Brahmakumar, and M. T. Sebastian, Int. J. Appl. Ceram. Technol. **11**, 919 (2014).
[5]Y. Yuan, S. R. Zhang, X. H. Zhou, and E. Z. Li, Mater. Chem. Phys. **141**, 175 (2013).
[6]T. Li, J. Chen, H. Dai, D. Liu, H. Xiang, and Z. Chen, J. Mater. Sci.: Mater. Electron. **26**, 312 (2015).
[7]Y. Yuan, Y. R. Cui, K. T. Wu, Q. Q. Huang, and S. R. Zhang, J. Polym. Res. **21**, 366 (2014).
[8]K. P. Murali, S. Rajesh, O. Prakash, A. R. Kulkarni, and R. Ratheesh, Composites, Part A **40**, 1179 (2009).
[9]M. Kubo, X. Li, C. Kim, M. Hashimoto, B. J. Wiley, D. Ham, and G. M. Whitesides, Adv. Mater. **22**, 2749 (2010).
[10]S. Koulouridis, G. Kiziltas, Y. J. Zhou, D. J. Hansford, and J. L. Volakis, IEEE Trans. Microwave Theory Tech. **54**, 4202 (2006).
[11]C. M. Shah, S. Sriram, M. Bhaskaran, M. Nasabi, T. G. Nguyen, W. S. T. Rowe, and A. Mitchell, J. Microelectromech. Syst. **21**, 1410 (2012).
[12]M. Amjadi, A. Pichitpajongkit, S. Lee, S. Ryu, and I. Park, ACS Nano **8**, 5154 (2014).
[13]P. Yi, R. A. Awang, W. S. T. Rowe, K. Kalantar-zadeh, and K. Khoshmanesh, Lab Chip **14**, 3419 (2014).
[14]M. A. Ali, S. Srivastava, P. R. Solanki, V. Reddy, V. V. Agrawal, C. Kim, R. John, and B. D. Malhotra, Sci. Rep. **3**, 2661 (2013).
[15]M. Nour, K. Berean, S. Balendhran, J. Z. Ou, J. Du Plessis, C. McSweeney, M. Bhaskaran, S. Sriram, and K. Kalantar-zadeh, Int. J. Hydrogen Energy **38**, 10494 (2013).
[16]Y. C. Chen, H. C. Lin, and Y. D. Lee, J. Polym. Res.-Taiwan **10**, 247 (2003).
[17]L. K. Namitha, J. Chameswary, S. Ananthakumar, and M. T. Sebastian, Ceram. Int. **39**, 7077 (2013).
[18]J.-W. Zha, Z.-M. Dang, W.-K. Li, Y.-H. Zhu, and G. Chen, IEEE Trans. Dielectr. Electr. Insul. **21**, 1989 (2014).
[19]T. Li, J. Chen, H. Dai, D. Liu, H. Xiang, and Z. Chen, J. Mater. Sci.: Mater. Electron. **26**, 312 (2014).
[20]Y. Hu, Y. Zhang, H. Liu, and D. Zhou, Ceram. Int. **37**, 1609 (2011).
[21]K. P. Murali, S. Rajesh, O. Prakash, A. R. Kulkarni, and R. Ratheesh, Mater. Chem. Phys. **113**, 290 (2009).
[22]M. T. Sebastian and H. Jantunen, Int. J. Appl. Ceram. Technol. **7**, 415 (2010).
[23]D. Sun, B.-B. Li, and Z.-L. Xu, Korean J. Chem. Eng. **30**, 2059 (2013).
[24]G. J. Hayes, J. H. So, A. Qusba, M. D. Dickey, and G. Lazzi, IEEE Trans. Antennas Propag. **60**, 2151 (2012).
[25]N. S. Broyles, K. N. E. Verghese, S. V. Davis, H. Li, R. M. Davis, J. J. Lesko, and J. S. Riffle, Polymer **39**, 3417 (1998).
[26]M. Lin and M. N. Afsar, in *IEEE MTT-S International Microwave Symposium Digest, San Francisco, CA, 11 June–16 June 2006*, pp. 1630–1633.
[27]S. Thomas, V. Deepu, S. Uma, P. Mohanan, J. Philip, and M. T. Sebastian, Mater. Sci. Eng., B **163**, 67 (2009).
[28]See supplementary material at http://dx.doi.org/10.1063/1.4945037 for supplementary information document.
[29]L. Ramajo, M. Reboredo, and M. Castro, Composites, Part A **36**, 1267 (2005).
[30]D. C. Dube, M. T. Lanagan, J. H. Kim, and S. J. Jang, J. Appl. Phys. **63**, 2466 (1988).
[31]G. Subodh, M. Joseph, P. Mohanan, and M. T. Sebastian, J. Am. Ceram. Soc. **90**, 3507 (2007).
[32]Y. Rao, J. Qu, T. Marinis, and C. P. Wong, IEEE Trans. Compon. Packag. Technol. **23**, 680 (2000).
[33]P. S. Anjana, V. Deepu, S. Uma, P. Mohanan, J. Philip, and M. T. Sebastian, J. Polym. Sci., Part B: Polym. Phys. **48**, 998 (2010).
[34]A. Tropmann, L. Tanguy, P. Koltay, R. Zengerle, and L. Riegger, Langmuir **28**, 8292 (2012).
[35]W. Chassé, M. Lang, J.-U. Sommer, and K. Saalwächter, Macromolecules **45**, 899 (2012).
[36]K. J. Berean, J. Z. Ou, M. Nour, M. R. Field, M. M. Y. A. Alsaif, Y. Wang, R. Ramanathan, V. Bansal, S. Kentish, C. M. Doherty, A. J. Hill, C. McSweeney, R. B. Kaner, and K. Kalantar-zadeh, J. Phys. Chem. C **119**, 13700 (2015).
[37]S. H. Yoo, C. Cohen, and C.-Y. Hui, Polymer **47**, 6226 (2006).
[38]S. Candau, J. Bastide, and M. Delsanti, Adv. Polym. Sci. **44**, 27 (1982).